GYROKINETIC SIMULATIONS AND ANALYSIS OF PEDESTALS

M. KOTSCHENREUTHER, X. LIU, D.R. HATCH, S.MAHAJAN, L. ZHENG
University of Texas at Austin
Austin, USA
Email: mtk@austin.utexas.edu

A. DIALLO
Princeton Plasma Physics Laboratory
Princeton, USA

R. GROEBNER and the DIII-D TEAM
General Atomics
San Diego, USA

C. F. MAGGI, C. GIROUD, F. KOECHL, V. PARAIL, S. SAARELMA, and JET CONTRIBUTORS*
Culham Centre for Fusion Energy, Culham Science Centre
Abingdon, UK
*See the author list of X. Litaudon et al 2017 Nucl. Fusion 57 102001

A. CHANKIN
Max-Planck-Institut für Plasmaphysik
Garching bei München, Germany

Abstract

Fusion performance in tokamaks hinges critically on the efficacy of the Edge Transport Barrier (ETB) at suppressing energy losses. For the first time, the instabilities that cause the residual unquenched losses in the ETB of many of todays experiments have been identified from the "transport fingerprints" of multiple widely posited candidates. Specific drift instabilities, rather than magnetohydrodynamic ones, dominate the energy losses. The analysis unifies and explains previously disparate experimental observations on multiple devices, and is applied in detail to two DIII-D ETBs. I-modes on C-mod are also examined. Also, a combined analytic and computational gyrokinetic approach is developed to address the question of the scaling of pedestal turbulent transport with arbitrary levels of ExB shear. Extensive numerical (gyrokinetic) simulations demonstrate that pedestal modes respond to shear suppression very much like the predictions of a basic analytic decorrelation theory. The quantitative agreement between the two provides a new dependable, first principles (physics based) theoretical framework to predict the efficacy of shear suppression in burning plasmas that lie in a low-shear regime not accessed by present experiments. This regime has been examined extensively. Due to strong gradients and geometrical effects in the pedestal, Ion Temperature Gradient/ Trapped Electron modes are not curvature-driven like the core instabilities, leading to crucial differences from core-like modes. A Simplified KInetic Model (SKIM), benchmarked with gyrokinetic simulations, provides a basis for optimization of transport barriers in burning plasmas and core plasmas, for both axisymmetric and 3D gemetries.

1. INTRODUCTION

Ever since its experimental discovery, the H-mode [1] has been the centerpiece of strategies for energy gain from fusion. This is due to its highly boosted energy confinement time τ_E = Plasma stored energy/ Heating power. High τ_E is the primary requirement for fusion gain, and it is high in an H-mode because an Edge Transport Barrier (ETB, aka pedestal) arises where most instabilities are quenched by velocity shear. Residual instabilities in the ETB act to confound the desire to confine energy. In fact, they determine the denominator of τ_E: core profiles are typically "stiff", so they are weakly dependent on heating power but strongly dependent on the pedestal. Thus, the heating power to sustain the core is essentially the heating power to sustain the pedestal. This, in turn, is determined by the instabilities causing residual energy losses in the barrier.

Major progress has been made in understanding this transport 1) For the first time, the instabilities that likely dominate energy transport in todays experimental pedestals have been identified from the "transport fingerprints" of multiple widely posited candidates. Micro-Tearing Modes (MTM) and Electron Temperature Gradient (ETG) modes usually dominate. The analysis is applied in detail to two DIII-D ETBs, and is also applied to pedestals from JET, ASDEX-U, and C-mod. It unifies and explains previously disparate experimental

observations on multiple devices. MHD-like modes, i.e. KBM, might dominate particle transport. 2) Extensive simulations demonstrate that the suppression of ITG turbulence by ExB shear, a requirement for the existence of the pedestal, is well explained by previous analytic theories; the low velocity shear in some burning plasma regimes may pose a serious problem, and 3) The physical nature of ITG/TEM modes in transport barriers has been elucidated, and differs in important ways from core-like modes. A theoretical framework is developed, which reveals regimes of greatly weakened instability, and provides a framework for transport optimization.

2. IDENTIFICATION OF INSTABILITES BY THEIR TRANSPORT "FINGERPRINTS"

Gyrokinetic simulations have been applied to pedestals by innumerable authors, revealing candidate instabilities that have been posited to cause energy losses in the ETB: ideal MHD-like modes (including Kinetic Ballooning Modes KBM [2-9]), Electron Temperature Gradient (ETG) modes [8-15], Micro-Tearing Modes (MTM) [13,15-17] and Ion Temperature Gradient/Trapped Electron Modes (ITG/TEM) [10,14,15,17-19].

The defining feature of a pedestal is its high velocity shear, so residual transport can only be caused by modes that resist shear suppression. Gyrokinetic simulations and analytical arguments show that the modes that satisfy this are: MHD-like (e.g. KBM), Micro-Tearing Modes (MTM) and Electron Temperature Gradient (ETG) modes. The instabilities ITG/TEM are quite susceptible to shear suppression, but have been found to be important in low shear regimes, so we consider them as well.

Their qualitatively different dynamics implies

1) Very different stability and transport trends
2) Very different mode frequencies ω in the plasma frame.
3) Very different relative effects on various transport channels.

For the first time, we use 3) as a "fingerprint" to identify ETB instabilities. First, we define diffusivities as the ratio of the flux Γ_s to the gradient, for each species, so $D_s = \Gamma_s/(dn_s/dr)$, and $\chi_s = Q_s/(dT_s/dr$. Based on analytical arguments and simulations, the transport ratios for the various modes are:

TABLE 1: FINGERPRINTS OF MODES RESISTANT TO VELOCITY SHEAR SUPPRESSION

Mode type	χ_i / χ_e	D_e / χ_e	D_Z / χ_e
MHD-like	~1	~2/3	~2/3
MTM	~1/10	~1/10	~1/10
ETG	~1/10	~1/20	~1/20

TABLE: 1: FINGERPRINTS OF MODES SUSCEPTIBLE TO VELOCITY SHEAR SUPPRESSION

Mode type	χ_e/χ_i	$D_e/(\chi_i+\chi_e)$	$D_Z/(\chi_i+\chi_e)$
ITG/TEM	1/4 - 1	-1/10 – +1/3	~1

The results above are not qualitatively surprising, but, as we will see, they have major consequences. Hence we have taken considerable effort, both analytically and via simulation, to verify the results in the table. The MHD-like modes (including KBM) cause very comparable diffusivities in <u>all</u> channels, and no pinches. The MTM and ETG, on the other hand, cause almost exclusively electron thermal transport. ITG/TEM are more complex, but nonetheless, they can be characterized as causing thermal transport in both electrons and ions and substantial impurity transport. Electron particle transport, depending on parameters, can vary from being moderately diffusive to having a weak pinch ($D_e/(\chi_i+\chi_e)$ is slightly negative).

Let us apply these concepts to a range of experimental observations.

Ion heat transport: Transport analysis of pedestals on ASDEX-U find that the total χ_i is close to neoclassical, χ_{neo}, for a dataset of 13 shots spanning collisionality [20], and similarly for a carefully analyzed DIII-D case [21]. One often finds $\chi_e >> \chi_i - \chi_{neo}$, i.e., the anomaly in the ion transport is much less than the anomalous electron transport. Whenever $\chi_e >> \chi_i - \chi_{neo}$, most anomalous energy transport must come from modes that, preferentially and predominantly, act on the electron thermal channel producing χ_{anom_e}. This is impossible if MHD-like modes dominated turbulent energy losses (and similarly for ITG/TEM): ion transport would

strongly deviate from the neoclassical value. Only MTM and/or ETG are potential culprits for the anomalous energy transport.

Impurity transport: The inter-ELM impurity transport is estimated in the literature to be neoclassical [22,23], with an impurity pinch. Detailed comparisons on ASDEX find good agreement, concluding "turbulent transport was of negligible importance to impurity transport" [22]. ELMs are widely inferred to be primarily responsible for preventing a secular rise in impurity content from the neoclassical pinch. ELMs are an MHD instability. Even though they *expel a minority of the plasma heating power*- (estimated as ~ 20-40% on time average [24]) they are apparently *much more effective at expelling impurities* than the inter-ELM transport, which is responsible for considerably more energy loss. If MHD-like modes were responsible for most energy loss, why would an MHD instability in the form of an ELM be critically necessary to expel high Z impurities, if the inter-ELM MHD instability were operative even more strongly (i.e., expelled considerably more energy)? If inter-ELM energy transport were dominated by MTM and ETG, *neither of which expels impurities*, then ELMs would, indeed, be needed.

Hence, applying the transport fingerprint to the impurity channel leads us to arrive at the same conclusions as with the ion thermal channel: MTM and/or ETG are responsible for the anomalous transport, not KBM.

Electron particle transport: The inferred diffusivity (defined as above), based on source estimates, has been found to imply D_e/χ_e is small on several devices [21,25]. Here we highlight calculations for JET. Estimates using JINTRAC for shots in the H-mode phase for 79668 and 79688 [26], and 84794 [27] and using EDGE2D [25] for 92168 and 92174 find that in the mid-pedestal region $D_e/(\chi_e+\chi_i) \sim 0.07$-$0.09$ or less. This is inconsistent with MHD-like modes being the major energy loss agent (in which case $D_e/(\chi_e+\chi_i) \sim 1/3$ would pertain).

Note that it is possible that MHD-like modes might be operative and enforce marginal stability of the pressure profile $\sim n (T_e+T_i)$ by acting through the electron density channel with a small D_e, and creating only a small χ_e and χ_i, in all the cases above. So these arguments do not contradict the essential assumptions of EPED [2,3].

For all of these shots the gross parameters are similar to those in simulations that find that ITG/TEM modes are suppressed on JET to the point where they are not a dominant total energy tranport channel. Presuming this is so, the dominant energy loss agents must, again, be MTM and/or ETG. Profile differences might be significant, so ITG/TEM might be significant and only be partially supressed, so they too are candidates (such modes can give small $D_e/(\chi_e+\chi_i)$.)

The effects of RMP: Surprisingly, RMPs provide further evidence. This is because, when the self-consistent plasma response is included, they can be considered as externally seeded MHD-like instabilities in the steep gradient region. The reason for this is as follows. Of course, RMPs are static in the lab frame. However, the large pedestal E_r and ExB Doppler shift implies that RMPs have $\omega \sim$ ion diamagnetic ω_i^* *in the plasma frame*, as is expected for ideal MHD-like modes. Analytical calculations below show this similarity implies the self-consistent plasma response gives $\delta E_{\|} \sim 0$ for the RMP in the steep gradient region. And this implies the transport fingerprint of RMP will be the same as an MHD-like instability in the steep gradient region.

The crucial experimental observation pertinent to applying the fingerprint is this: RMPs are observed to result in density pump-out, reduction in pedestal n_e and prevention of secular impurity build-up, but do not reduce pedestal T_e or T_i in the steep gradient region [28-31]. This is fully in accord with all the results above.

Occam's Razor: In the spirit of Occam's razor, the weak density source is the single ansatz, which implies all the disparate observations above.

Consider an idealized thought experiment. As the pressure gradients increase following an ELM, an MHD-like mode (e.g. KBM) becomes active, causing comparable diffusivity in all channels. Since the n_e source is weak, it is much more strongly affected- so its evolution, mainly, enforces MHD marginal stability (as in EPED [5,6]). *Since the density source is weak, a small D_e will suffice to strongly affect the density profile. But the χ_e and χ_i, needed to saturate the evolution of T_e and T_i are much larger than D_e, since those channels are much more strongly driven. The requisite χ_e and χ_i, therefore, must arise from MTM, ETG and neoclassical. If MHD-like modes did cause most energy transport, n_e would quickly collapse, stabilizing them.*

Summary: The reader should appreciate the strikingly consistent pattern of results presented. On ASDEX-U, DIII-D, JET and Alcator C-mod, observations on the areas above are inconsistent with MHD-like modes

dominating energy transport, but is only consistent with MTM and/or ETG taking that role. (ITG/TEM are possibilities as well on JET). The scope of this pattern leads one to the judgement that these conclusions are likely typical of ELMy H-modes on present tokamaks (at least for normal aspect ratio, as in the observations).

3. ANALYTIC DERIVATION OF TRANSPORT FINGERPRINTS

The transport fingerprint of MHD-like modes, and of MTM can be obtained from fundamental theoretical considerations implicit in the drift-kinetic Maxwell system pertaining to the physical parameters of the pedestal. We use Quasi-Linear Theory (QLT) to compute the ratio of transport in different channels. In the core, QLT has been used successfully to compute these ratios [32-34], and it is used for these ratios in the TGLF model for core transport, which has been widely benchmarked [35].

We start with the drift-kinetic equation of Hazeltine derived in a maximal ordering [36] to allow treatment of both drift and MHD-like modes, and to allow strong profile variations over the mode extent as in ETBs. To compute the quasilinear fluxes in different channels, one subtracts out the "purely convective" part of the perturbed distribution δf_s. Simple algebra gives, for the deviation from that convective response, $\delta f_{dev\,s} = \delta f_s - \delta f_{conv\,s}$, the kinetic equation

$$-i\omega_{pl}\,\delta f_{dev\,s}+(\mathbf{v_d}+v_{||}\,\mathbf{b})\cdot\nabla\delta f_{dev\,s}+C(\delta f_{dev\,s}) = (1-\omega_s^*/\omega_{pl})\,(q_s\,\delta E_{||}/T_s)v_{||}\,f_{Ms} + (q_s\,\mathbf{v_d}\cdot\nabla\,\delta f/T_s)\,(\omega^*/\omega_{pl})\,f_{Ms}$$

in standard notation: ω^* is the diamagnetic frequency, δ refers to fluctuations, $v_{||}$ and $\mathbf{v_d}$ are the parallel and drift velocity, ω_{pl} is frequency ω in the local plasma frame (including $\mathbf{v_{0ExB}}$ Doppler shift), $\omega_{pl} = \omega - \omega_{ExB}(r)$ (r is a flux label), and $\delta E_{||} = -\mathbf{b}\cdot\nabla\delta\phi - i\,\omega_{pl}\,\delta A_{||}$.

The deviations from purely convective response are, thus, driven by terms $\sim \delta E_{||}$ *and* $\sim$ *(1/* ω_{pl}*)* $\mathbf{v_d}\cdot\nabla$. For steep gradients, and modes with $\omega \sim \omega^*$, the latter term is very small ~ L/R, where L is the equilibrium gradient scale length. *So in the pedestal, if* $\delta E_{||} \sim 0$*, as in MHD-like modes,* δf_s is mainly $\delta f_{conv.}$

If the primary behavior is ExB convection of all species, we expect that all channels have similar transport diffusivities; computed quasi-linear fluxes confirm the expectation. (And furthermore, there is only diffusion, with no pinch). These general arguments are not strongly dependent on details of the mode structure or type.

Further analysis in the steep gradient ordering shows there is a connection between frequency in the plasma frame ω_{pl} and the magnitude of $\delta E_{||}$. For electromagnetic modes in a pedestal, $\delta j_{||}$ tends to be "too large"- the tilt δB_r in the direction of the strong ETB gradient gives a large parallel gradient, and hence large $\delta j_{||}$ and also $\nabla_{||}\delta j_{||}$, that is to big to be balanced by polarization current contribution $\nabla\cdot\,\delta j_{\perp}$. When this is so, charge builds up to produce an electrostatic potential so that $\nabla_{||}\delta\phi$ cancels the inductive $\delta E_{||}$; with small $\delta E_{||}$, the $\delta j_{||}$ becomes small enough for quasineutrality to be satisfied. Using analysis very similar to that in the kinetic theory of tearing modes [37], for a pedestal ordering, we obtain the criterion for small $\delta E_{||}$ as

$$(m_i/m_e)(L/L_s)^2 << [(\omega_{pl} - \omega_e^*)/(\omega_{pl}-\omega_i^*)](\omega_e^*/\omega_{pl})^2 \qquad \text{Eq(19)}$$

Where L_s is the magnetic shear length. In the steep gradient region, the LHS is small because the gradient scale length L is small. Hence, unless the perturbation has $\omega_{pl} \sim \omega_e^*$, $\delta E_{||}$ will be small there. Thus, the mode frequency in the plasma frame is extremely important for the transport fingerprint; unless $\omega_{pl} \sim \omega_e^*$, as occurs for an MTM, all diffusivities should be equal for a magnetic mode.

This also applies to an RMP in the steep gradient region; hence, the transport response and fingerprint will be the same as an MHD-like mode. (Inside the top of the pedestal, where L is much larger, this is not so: islands can be induced, giving predominantly electron thermal transport.)

The transport fingerprints for the instabilities above also be computed by gyrokinetic simulation of experimental pedestals on DIII-D, JET-C and JET-ILW, and Alcator C-mod. The results corroborate the general analytic arguments above. We now turn to a detailed consideration of two DIII-D cases.

4. DETAILED CONSIDERATION OF TWO DIII-D DISCHARGES

We first consider DIII-D shots 153674, which has an extensive diagnosis of inter-ELM behavior [4].

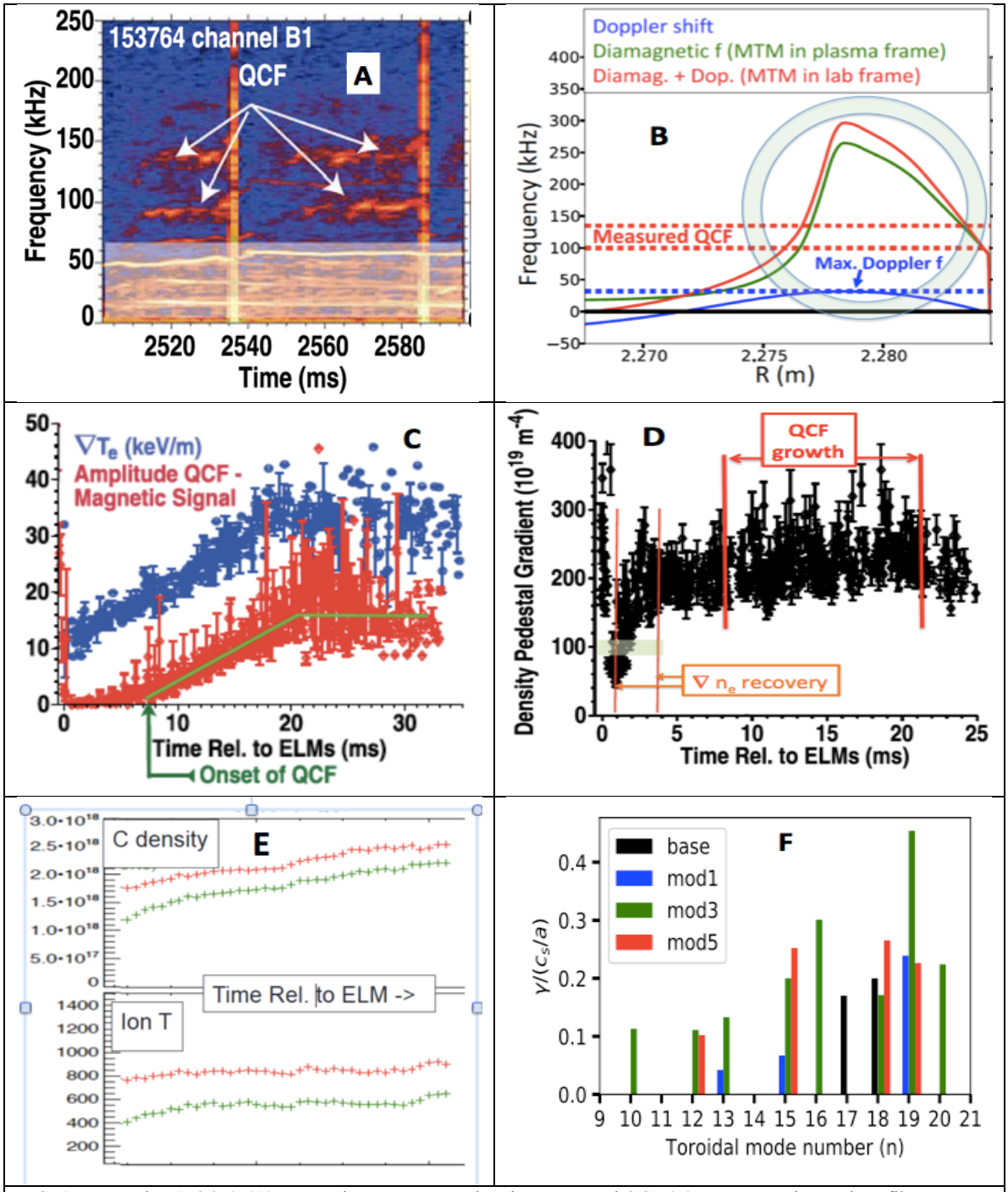

FIG. 1 DIII-D shot 153674. (A) Magnetic spectrogram showing measured QCF (B) From experimental profiles, frequencies for: Doppler shift (ω_{ExB}), ω_e*, and the QCF. The circle shows the experimentally inferred QCF position range (C) Inter-ELM evolution of T_e gradient and QCF amplitude showing strong correlation (D) Evolution of density gradient showing no affect of growing QCF on ∇n_e (F) Evolution of T_i and n_C after an ELM, for a typical ELM cycle, showing no discernable affect of growing QCFs. Note the difference between values on two cords is proportional to the average gradient between them. Hence, the gradient of T_i and n_C between the cords is apparently unaffected by the growing QCF. Over-all behaviour is consistent with MTMs, but inconsistent with KBMs (F) Instability spectrum for global simulations with GENE, for variations of the profile within the error bars. Only MTM were unstable. Discrete instability spectrum in n should give QCF as observed. Case mod5 has a dominant instability at n=15, close to observations (n~13-14), and a subdominant mode at n=12, also qualitatively similar to observation.

Magnetic probes and Beam Emission Spectroscopy (BES) measure a Quasi-Coherent Fluctuation (QCF). The mode that is most strongly correlated with T_e evolution has f ~140kHz, in the electron direction. See Fig. 1a. As noted above, it is crucial to establish f in the plasma frame. In Fig 1b, we plot the Doppler shift from the measured E_r and k_θ(the latter from BES), and ω_e^*. Even for the *maximum* $\omega_{ExB}(r)$, the Doppler shift is much less

than the lab f- *hence, f must be in the electron direction in the plasma frame, wherever the mode is "located"*. The measured f is consistent with ω_e* for the experimentally inferred position of the mode, but with a large uncertainty.

As emphasized in the published description of this shot [4], the growth of the magnetic signals is strongly correlated with the evolution of the T_e gradient (see Fig. 1c); they grow and saturate together, strongly suggesting that the QCF is driven by it, and/or, causes substantial transport in that channel. For mode identification, it is just as significant that the growing QCF apparently has no effect on the evolution of the density gradient. See Fig. 1d: the growing QCF has no apparent affect on ∇n_e. Furthermore, pedestal measurements of T_i and the impurity density of Carbon n_C are shown in Fig. 1d, for a representative inter-ELM period. Data from two separate chords in the pedestal are plotted. The difference in the signal between the cords is proportional to the average plasma gradient of the quantity between them and this is very nearly constant in time for both T_i and n_C. A growing KBM would evolve to enforce marginal stability by substantial comparable transport in all channels. However, this QCF only affects ∇T_e. This is consistent with an MTM, not a KBM.

Local simulations [38] with GENE [39,40] find MTM instabilities for k_x values $\neq 0$. Global simulations for the given equilibrium find a global MTM, but with an outboard midplane k_θ that is ~ 1.5 times higher than the measures value 0.18-0.2 cm^{-1} (corresponding to n ~ 13-14.) The pedestal profiles were modified within the error bars and new self-consistent MHD equilibria were computed. We show results for three cases labelled mod1,mod3 and mod5. Note the strong sensitivity of the unstable spectrum. For mod5, the spectrum is close to observations, but with a frequency f that is 2x too high. Nonlinear simulations of this case find a downshift to within ~ 40% of the observation. The nonlinear heat flux from this MTM is 0.6 MW, and there is 1.4 MW of heat loss from nonlinear ETG, so a combination of MTM and ETG is close to the power loss of ~3 MW.

We now turn to shot DIII-D 98889, where an extremely valuable transport analysis is already available [24]. A summary of the conclusion is as follows.

a) The inferred χ_e is about twice the χ_i
b) The latter is χ_i roughly consistent with neoclassical or paleoclassical expectations.
c) The inferred electron diffusivity *D_e is an order of magnitude lower than χ_e*

From these results, MHD-like modes cannot be predominantly responsible for energy transport, by the same arguments delineated in section 2. Both the smallness of D_e, and separately, the relative smallness of the ion anomaly $\chi_i - \chi_{neo} << \chi_e$, each preclude MHD-like modes from being the dominant energy loss.

We expect that ITG/TEM modes are probably strongly suppressed in this pedestal. Even allowing for the possibility that they are active, they would give a large χ_i anomaly that is not observed. Hence, the only consistent candidates for anomalous energy transport are MTM and/or ETG.

A magnetic spectrogram for this shot, shows QCFs that are comparable to those in Fig. 1a and 1b: the frequencies in the plasma frame must be in the electron direction and ~ ω_e* (even accounting for the Doppler shift from the measured E_r). Hence , we conclude these fluctuations are MTM.

Local linear simulations find that MTM are the most unstable modes. As in the case of shot 153674/5, the global instability spectrum finds MTM instabilities at discrete mode number n (n=16,18 and 21), separated by weakly unstable electrostatic TEM/ETG modes. This would tend to give quasi-coherent magnetic fluctuations, as in the spectrogram. The f values for n =16 and 18 are about 1.5 times the high f bands on the magnetic spectrogram. Nonlinear simulations of these modes show a nonlinear downshift of the frequency, to within ~ 40% of the observed values. The heat flux from MTM is 2.6 MW, or slightly more than the transport estimate of 1.8 MW.

5. VELOCITY SHEAR SUPPRESSION OF ITG MODES

Velocity shear suppression of electrostatic drift instabilities is necessary for low pedestal transport in present devices to allow the pedestal gradients to be maintained. This is especially noteworthy in view of the fact that the velocity shear, based on the usual neoclassical expectations, scales as ρ*, so that shear suppression in a pedestal such as ITER's is significantly less than on present experiments. Gyrokinetic simulations using GENE have found that such drift instabilities, ITG/TEM modes, can potentially produce unacceptable energy transport in ITER-like pedestal equilibria. Here, similar simulations using GENE for find excellent agreement with the decorrelation theory of Zhang and Mahajan [41]. Very extensive parameter scans were carried out to enable

detailed comparisons with the theory. (To do this at acceptable computational cost, adiabatic electrons were assumed.) A unique feature of the theory is that it spans the regimes of strong and weak shear.

Despite its relative simplicity, the theory- simulation agreement is very good over the entire range. Thus we have the makings of a first-principles, physics-based theory of turbulence suppression (via shear flow) that can be exploited to estimate/predict turbulent transport in regimes that have not been experimentally probed yet. In a controlled ρ^* scan (velocity shear ~ ρ^*), the suppressed heat flux from ITG modes scales much more poorly than gyro-Bohm. It is nearly independent of ρ^*, so it may become relatively quite large, relative to gyroBohm expectations, at the low ρ^* of burning plasmas.

In view of these results, the most promising route to optimized pedestal performance in low velocity shear regimes is by minimizing ITG growth rates. These results, and those in section 1-4 above, imply that gyrokinetic simulations of drift-class modes are essential for projecting pedestal performance in burning plasma regimes.

6. THE PHYSICS OF ITG/TEM MODES IN PEDESTALS

A comprehensive investigation of the properties of electrostatic modes has been undertaken. Gyrokinetic simulations together with analytic theories have been used to understand the physics of such modes in pedestals. These modes are in a quite different physical regime from core-like parameters, so the dominant physical processes and parametric dependencies are often very different. Unique properties of this regime include 1) Curvature is a relatively weak drive, rather, parallel resonance effects are predominant- the opposite of core-like modes 2) The radial scales of the modes can sometimes be far shorter than the poloidal scale, likely making velocity shear suppression more difficult 3) mode frequencies can be a very small fraction of the ion diamagnetic frequency 4) As in the core, electron trapped particle effects are significantly destabilizing. In view of the low frequency, collisional detrapping is often faster, even for burning plasmas, so collisions reduce this. So the TEM drive is the dissipative kind. 5) A consequence of the subdominant curvature drive is that instability thresholds are mainly in terms of η = d logT/d log n; quite different from the core, where thresholds are ~ R/L_T (L_T is the T gradient scale length) 6) Because of the primacy of parallel resonance effects, the ITG drive reverts to strong damping when η_i drops below a threshold. Thus, ITG/TEM modes have a window of near stability for η_i ~ 1-2. 7) Parallel electron resonances lead to a strong destabilization for lower η_e However, this is suppressed electromagnetically at very low beta (~10^{-4}–10^{-3}); purely electrostatic simulations sometimes do not suffice.

These properties are understood analytically by the construction of a Simplified KInetic Model (SKIM). Starting with an exact variational formulation of the dispersion relation, a sequence of judicious simplifications are made to convert this to a remarkably simple form, which is close to very early analytic theories. Complex geometric effects enter as a small number of intuitive parameters defined by eigenfuction averages of equilibrium quantities. The SKIM agrees well with GENE simulations, for parameters from the core to the pedestal. It clarifies the transition of the physics from core-like to pedestal-like regimes.

An important aspect that is clarified by SKIM is the strong influence of the geometrical structure of the effective curvature drive, which can be strongly influenced by the *poloidal* magnetic field (which is modified by the pedestal bootstrap current and pressure gradient), even though the dominant curvature is from the toroidal field. For pedestal regimes it becomes geometrically impossible for the mode to be driven by curvature; any mode structure that localizes to the limited bad curvature extent will inevitably lead to overwhelming parallel resonance effects. Short gradient scale lengths of n and T accentuate this, but the primary effect in realistic geometries is from the modified effective curvature relative to the core.

Using SKIM, one can predict regimes of reduced transport from the interplay of geometrical effects with plasma parameters, which would not otherwise be obvious. These can then be verified by simulation. While the SKIM framework above was developed for transport barriers, it applies to core-like parameters as well. It opens up possibilites for novel types of geometric optimization. These concepts are quite general, and apply to both axisymmetric and 3D configurations, and so should be pertinent to stellarator optimization as well.

ACKNOWLEDGEMENTS

This material is based upon work supported by the U.S. Department of Energy grant DE-FG02-04ER54742, the National Energy Research Scientific Computing Center and the Texas Advanced Computing Center.

This work has been carried out within the framework of the EUROfusion Consortium and has received funding from the EURATOM research program 2014-2018 under grant agreement No. 633053. The views and opinions expressed herein do not necessarily reflect those of the European Commission.

This material is based upon work supported by the U.S. Department of Energy, Office of Science, Office of Fusion Energy Sciences, using the DIII-D National Fusion Facility, a DOE Office of Science user facility, under Awards DE-FC02-04ER54698. DIII-D data shown in this paper can be obtained in digital format by following the links at https://fusion.gat.com/global/D3D_DMP.

REFERENCES

[1] Wagner F. , Plasma Phys. Control. Fusion 49 (2007)
[2] P.B. Snyder, et. al., Nucl. Fusion 49 (2009) 085035
[3] P.B. Snyder, et. al., Nucl. Fusion 51 (2011) 103016
[4] A. Diallo, R. J. Grobner, T. L. Rhodes, D. J. Battaglia, D. R. Smith, et. al., Phys. Plasmas 22, 056111 (2015)
[5] Wan W., Parker S.E., Chen Y., Groebner R.J., Yan Z., Pankin A.Y. and Kruger S.E. 2012 Phys. Plasmas 20 055902
[6] D Dickinson, S Saarelma, R Scannell, A Kirk, C M Roach, H.R. Wilson, Plas. Phys. Control. Fusion 53 (2011) 115010
[7] D. Dickinson, C. M. Roach, S. Saarelma, R. Scannell, A. Kirk, and H. R. Wilson, PRL 108, 135002 (2012)
[8] D.R. Hatch, D. Told, F. Jenko, H. Doerk, M.G. Dunne, E. Wolfrum, et. al., Nucl. Fusion 55 (2015) 063028 PR
[9] J. M. Canik, et. al., Nucl. Fusion 53 (2013) 113016
[10] D. Told, F. Jenko, P. Xanthopoulos, L. D. Horton, E. Wolfrum, et. al, Phys. Plasmas 15, 102306 2008
[11] F. Jenko, D. Told, P. Xanthopoulos, F. Merz, and L. D. Horton Phys. Plasmas 16, 055901 (2009)
[12] Daniel Told, Ph.D. Thesis Universität Ulm (2012)
[13] D.R. Hatch, M. Kotschenreuther, S. Mahajan, et. al., Nucl. Fusion 56 (2016) 104003
[14] M. Kotschenreuther, D.R. Hatch, S. Mahajan, Nucl. Fusion 57 (2017) 064001
[15] D.R. Hatch, M. Kotschenreuther, S. Mahajan, et. al., Nucl. Fusion 57 (2017) 036020
[16] D. Dickinson, et al., Plasma Phys. Control. Fusion 55 (2013) 074006
[17] S. Saarelma, M.N.A. Beurskens, D. Dickinson, L. Frassinetti, M.J. Leyland, et. al., Nucl. Fusion 53 (2013) 123012
[18] Chang et al Nucl. Fusion **57** (2017) 116023
[19] C. Zhao, T. Zhang, Y. Xiao, Physics of Plasmas **24**, 052509 (2017)
[20] E. Viezzer, E. Fable, M. Cavedon, C. Angioni, R. Dux, F.M. Laggner, et.al., Nucl. Fusion 57 (2017) 022020
[21] J. D. Callen, R. J. Groebner, et. al., Nucl. Fusion 50 (2010) 064004
[22] T. Pütterich, R. Dux, M.A. Janzer, R.M. McDermott, et.al, Journal of Nuclear Materials 415 (2011) S334–S339
[23] T. Sunn Pedersen, R.S. Granetz, A.E. Hubbard, I.H. Hutchinson, E.S. Marmar, et. al., 2000 Nucl. Fusion 40 1795
[24] A. Loarte ,et.al., Nucl. Fusion 54 (2014) 033007
[25] A. V. Chankin, D. P. Coster, R. Dux, Ch Fuchs, G. Haas, et.al., Plasma Phys. Control. Fusion 48 (2006) 839–868
[26] F. Koechl, A. Loarte, V. Parail, P. Belo, M. Brix, G. Corrigan, D. Harting, et. al. 2017 Nucl. Fusion 57 086023
[27] L. Horvath, C. F. Maggi, F. J. Casson, V. Parail, L. Frassinetti, et. al., Plasma Phys. Control. Fusion 60 (2018) 085003
[28] RM L. Cui, R. Nazikian, et. al., Nucl. Fusion 57 (2017) 116030
[29] G. R. McKee et. al., Nucl. Fusion 53 (2013) 113011
[30] R. Nazikian, et al., PRL 2015
[31] S Saarelma, A Alfier, Y Liang, L Frassinetti, M Beurskens, et. al. , Plasma Phys. Control. Fusion 53 (2011) 085009
[32] F. Jenko, T. Dannert and C. Angioni, Plasma Phys. Control. Fusion 47 (2005) B195–B206
[33] A. Casati, C. Bourdelle, X. Garbet, F. Imbeaux, J. Candy, F. Clairet, et. al., Nucl. Fusion 49 (2009) 085012
[34] C. Bourdelle, J. Citrin, B. Baiocchi, A. Casati, P. Cottier, et. al., Plasma Phys. Control. Fusion 58 (2016) 014036
[35] G. M. Staebler , J. E. Kinsey , and R. E. Waltz, Phy. Plasma 14 , 055909 (2007)
[36] R. D. Hazeltine, Plasma Physics, 15, (1973) 77
[37] J. F. Drake and Y.C. Lee, Physics of Fluids 20, 1341 (1977)
[38] Xing Liu, Ph.D. Thesis University of Texas at Austin 2018
[39] Jenko F., Dorland W., Kotschenreuther M. and Rogers B.N. Phys. Plasmas 7 1904 (2000)
[40] Görler T., Lapillonne X., Brunner S., Dannert T., Jenko F., Merz F. and Told D. 2011 J. Comput. Phys. 230 7053
[41] Y. Z. Zhang and S. M. Mahajan, Physics of Fluids B, **5**, (1993) 2000